

# Photoluminescence from a Bulk Defect near the Surface of an *n*-TiO<sub>2</sub> (Rutile) Electrode in Relation to an Intermediate of Photooxidation Reaction of Water

Y. Nakato,\* H. Akanuma, Y. Magari, S. Yae, J.-I. Shimizu, and H. Mori†

Department of Chemistry, Graduate School of Engineering Science, and Research Center for Photoenergetics of Organic Materials, Osaka University, 1-3 Machikaneyama, Toyonaka, Osaka 560, Japan

Received: September 27, 1996; In Final Form: March 24, 1997®

A photoluminescence (PL) band peaked at 840 nm is observed for an *n*-TiO<sub>2</sub> (rutile) electrode in aqueous electrolyte solutions when illuminated under a slight anodic bias and was previously explained as arising from an intermediate of photooxidation reaction of water on the *n*-TiO<sub>2</sub> electrode. The chemical structure and properties of the PL-emitting species have been investigated in the present work by measurements of photocurrent, photoluminescence, electroluminescence, and transient luminescence as well as inspection of the electrode surface by transmission electron microscopy. It is concluded that the PL band should be assigned to an electronic transition from the conduction band to the vacant level of HO• radicals present in a bulk defect (atomic gaps) near the *n*-TiO<sub>2</sub> (rutile) surface and that the radicals act as an intermediate of the photooxidation reaction of water. The results give confirmative evidence to our previously proposed new mechanism that the surface Ti–OH group cannot be oxidized by photogenerated holes, and thus the reaction in acidic solutions is initiated by the oxidation of Ti–OH or OH<sup>−</sup> in the bulk defect near the surface.

## Introduction

The electrochemical oxygen evolution and reduction are both key reactions in energy conversion technologies, but unfortunately they have fairly large overpotentials (or activation energies), leading to significant losses in the conversion efficiencies.<sup>1</sup> These reactions proceed at large positive potentials where most metal electrodes are covered with native oxide layers. Therefore, the elucidation of the mechanism of the reactions on metal oxide electrodes is very important for finding new efficient electrode materials.

In this respect, the mechanism of photooxidation reaction of water on an *n*-TiO<sub>2</sub> electrode<sup>2</sup> is interesting. A number of studies<sup>3–12</sup> have been made on the reaction, and it has been assumed in most cases that the reaction is initiated by the oxidation of surface Ti–OH group by photogenerated holes. On the other hand, we found previously that the *n*-TiO<sub>2</sub> (rutile) electrode showed a photoluminescence (PL) band peaked at 840 nm, which could be explained as arising from a surface reaction intermediate or a species closely related to it.<sup>13</sup> This enabled us to use in situ PL measurements for the mechanistic studies.<sup>13–15</sup> From detailed studies, we proposed a new mechanism that surface Ti–OH group cannot be oxidized by photogenerated holes and thus the reaction in acidic solutions is initiated by the oxidation of Ti–OH group or OH<sup>−</sup> ion present in a bulk defect (such as dislocations) near the surface.<sup>15,16</sup> The main scheme is shown in Figure 1 for later discussion. It is to be noted that our new mechanism does not exclude a possibility of the oxidation of surface species by the holes in neutral and alkaline solutions because a much more easily oxidized surface species than Ti–OH, such as Ti–O<sup>−</sup>, may be formed by deprotonation in the case of such solutions (the point of zero charge of rutile-type TiO<sub>2</sub> is about 5.5). The surface oxidation may also occur for anatase-type TiO<sub>2</sub> which has a wider band gap than rutile-type TiO<sub>2</sub>.

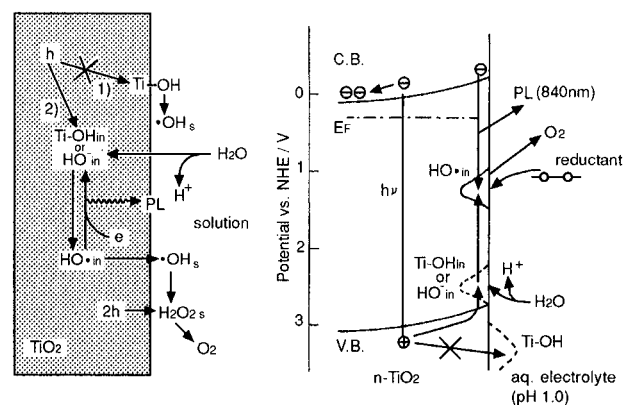


**Figure 1.** Schematic illustrations of a new mechanism for the photooxidation reaction of water on *n*-TiO<sub>2</sub> (rutile) in acidic solutions: CB, conduction band; VB, valence band; EF, Fermi level. Energy levels depicted by broken lines are only roughly estimated. Radiative recombination between HO•<sub>in</sub> and e<sup>−</sup><sub>CB</sub> occurs only under weak band bending.

The key of our new mechanism lies in that the rate constant for the oxidation of Ti–OH (or OH<sup>−</sup> ion) in the bulk defect by photogenerated holes is much higher than that for the oxidation of surface Ti–OH group, as verified theoretically.<sup>16</sup> In our model, the bulk defect is assumed to be a kind of narrow atomic gap and therefore Ti–OH or OH<sup>−</sup> ion in the bulk defect is present in the “naked” form, i.e., not hydrated by water molecules, contrary to the surface Ti–OH group which is strongly hydrated by water molecules of the solution. In other words, the Ti–OH or OH<sup>−</sup> ion in the bulk defect is mainly stabilized by the electronic polarization of TiO<sub>2</sub> crystal, whereas the surface Ti–OH group is largely stabilized by the orientational polarization of water molecules. Thus, the reorganization energy (and hence the activation energy) for electron transfer in Marcus theory is much less in the oxidation of the bulk species than in that of the surface species.<sup>17</sup> In this respect, our new mechanism is of much interest, opening a possibility of a new active path for electrode reactions.

However, a criticism to our new mechanism was later reported,<sup>3</sup> probably due to shortage of confirmative experimental

† Research Center for Ultra-High Voltage Electron Microscopy, Osaka University, Yamadaoka, Suita, Osaka 565, Japan.

\* To whom correspondence should be addressed. E-mail: nakato@chem.es.osaka-u.ac.jp. Fax: 81-6-850-6236.

® Abstract published in *Advance ACS Abstracts*, June 1, 1997.

evidence in our previous work. Moreover, we later found a paper<sup>18</sup> reporting that  $\text{Cr}^{3+}$  ions, contained in  $\text{TiO}_2$  as an impurity, emitted a PL band accidentally at the same wavelength (840 nm) as that observed by us. This also caused a criticism to our model in the interpretation of the luminescence bands of  $n\text{-TiO}_2$ .<sup>19</sup> Thus, we recently started systematic studies<sup>20,21</sup> on our new mechanism in order to obtain confirmative experimental evidence. We have reported in a previous paper<sup>21</sup> that the effect of alcohols added to the solution on the photocurrent in addition to the PL band at 840 nm gives clear evidence to our new mechanism if it can be assumed that the PL-emitting species is a bulk species. Thus, the main purpose of the present paper is to clarify the chemical origin and properties of the PL-emitting species and to show that it is a bulk species.

## Experimental Section

Single-crystal  $\text{TiO}_2$  (rutile) wafers,  $10 \times 10 \text{ mm}^2$  in area and 1.0 mm thick, cut perpendicular to the  $c$ -axis and having a purity of 99.99%, were obtained from Earth Jewelry Co., Ltd. They were polished with alumina powder of diameters 3.0, 1.0, 0.3, and  $0.1 \mu\text{m}$  successively (sometimes  $0.06\text{-}\mu\text{m}$  powder was used); etched in concentrated sulfuric acid containing 33 wt %  $(\text{NH}_4)_2\text{SO}_4$  at  $200\text{--}250^\circ\text{C}$  for 30 min; washed; annealed in air at  $1300^\circ\text{C}$  for 3–4 h; and then slightly reduced by heating at  $550\text{--}700^\circ\text{C}$  for 30 min under a stream of hydrogen for getting  $n$ -type semiconductivity, in the same way as before.<sup>20,21</sup> The resistivity ( $\rho$ ) of the  $n\text{-TiO}_2$  wafer was measured by painting indium–gallium alloy on both faces of the wafer. In the present work, samples of  $0.2\text{--}2.0 \Omega \text{ cm}$  were used. After the alloy was removed by immersing in an HCl solution, ohmic contact for electrode preparation was obtained by painting again indium–gallium alloy on one face of the wafer.

Photocurrent density ( $j$ ) vs potential ( $U$ ) curves were obtained with a commercial potentiostat and potential programmer, using a Pt plate as the counter electrode and an Ag/AgCl electrode as the reference electrode. Electrode illumination was usually performed by a 365-nm band from a 500-W high-pressure mercury lamp. Photoluminescence spectra were measured with a Jobin-Yvon H20 monochromator and a Hamamatsu Photonics R316 or R712 photomultiplier cooled at  $-20^\circ\text{C}$ .<sup>20,21</sup> PL intensity vs potential curves were measured simultaneously with the  $j\text{--}U$  curve measurements.

The structure of the electrode surface was investigated with a Hitachi H-9000 transmission electron microscope. Electrolyte solutions were prepared by use of water purified from deionized water with a Milli-Q Water Purification System. Chemicals of reagent grade were used without further purification. The electrolyte solution in the cell was in most cases stirred during measurements. The concentration unit,  $\text{mol/dm}^3$ , is abbreviated as M in the present work.

## Results

**Structure of a Bulk Defect near the Surface.** First, we describe briefly our reported results on which the present experiments are based. We recently found<sup>20</sup> that a “fresh”  $n\text{-TiO}_2$  electrode (i.e., an electrode just prepared by the procedures of polishing, etching, annealing, and hydrogen reduction as described in the experimental section) showed only a weak photocurrent and no PL in the first potential scan, but both the photocurrent and the PL intensity increased very much with time nearly in parallel to each other and finally reached the maxima when the potential scans were repeated under illumination in  $0.05\text{M H}_2\text{SO}_4$ . An example of such initial changes is shown in Figure 2A. (The result of Figure 2B is newly reported in the present paper and explained later.) The

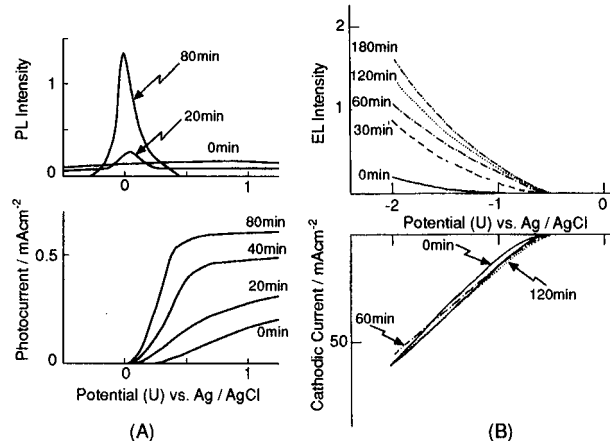


**Figure 2.** (A) Initial changes in the photocurrent ( $j_p$ ) and the PL intensity ( $I_{PL}$ ) for fresh  $n\text{-TiO}_2$  by illumination in  $0.05 \text{ M H}_2\text{SO}_4$ . (B) Changes in the EL intensity ( $I_{EL}$ ) and the cathodic current density ( $j_c$ ) for fresh  $n\text{-TiO}_2$  in a carbonate-buffered  $0.3 \text{ M Na}_2\text{SO}_4$  (pH 8.9) containing  $0.9 \text{ M H}_2\text{O}_2$  (stirred). The changes in  $I_{EL}$  were caused by the electrode activation pretreatment (i.e., the electrode illumination in  $0.05 \text{ M H}_2\text{SO}_4$ ). All of the values for time indicated in the figures represent the period of time of electrode illumination in  $0.05 \text{ M H}_2\text{SO}_4$ .

initial changes were in most cases accompanied by the formation of a lot of micropores (20–80 nm in diameter) at the electrode surface as confirmed by scanning electron microscopy.<sup>20</sup>

The above initial changes clearly indicate that our observing PL band at 840 nm is not arising from a  $\text{Cr}^{3+}$  impurity in  $\text{TiO}_2$  but from a species produced through interfacial electrochemical reactions. The above results also indicate that the  $n\text{-TiO}_2$  electrode is activated by the flow of anodic photocurrent in  $0.05 \text{ M H}_2\text{SO}_4$  due to photoetching, which occurs slightly and competitively with the photooxidation reaction of water. It is to be noted also that similar activation occurs even by chemical etching in (hot) concentrated  $\text{H}_2\text{SO}_4$ ,<sup>20</sup> which is usually used for cleaning of the  $\text{TiO}_2$  surface. Furthermore, once-activated  $n\text{-TiO}_2$  electrodes show the “active” characteristics (i.e., efficient  $j\text{--}U$  curves and strong PL) in other solutions, such as  $0.1 \text{ M HClO}_4$  and  $0.5\text{M Na}_2\text{SO}_4$ , in which no activation of fresh electrodes occurs. The activated state is kept for more than several weeks. From these features, it is probable that many studies reported thus far on  $\text{TiO}_2$  have been made unconsciously using such activated electrodes. We concluded previously<sup>20</sup> that such activation is due to the increase in the specific rate (cross section) of the photooxidation reaction of water, and it is not due to the increase in the area of the electrode surface by the pore formation. This is seen also from Figure 2A which shows the most prominent increase in the photocurrent in the region of recombination-controlled photocurrent between 0.0 and  $0.4 \text{ V vs Ag/AgCl}$ .

In the present work, in order to examine a possibility of whether a certain active reaction site (i.e., the “bulk defect” mentioned in the introduction section) is produced in the course of the illumination (photoetching) in  $0.05 \text{ M H}_2\text{SO}_4$ , we scratched the surface of the activated  $n\text{-TiO}_2$  electrodes with a diamond cutter and the obtained powder was inspected by transmission electron microscopy (TEM). The same experiments were done for nonactivated (not photoetched, fresh)  $n\text{-TiO}_2$  electrodes for comparison. Figures 3–5 show some examples of the TEM images. In general, the powder from the activated electrodes consisted of thin leaves of crystals (Figure 3). Also, most of the powder showed “moiré patterns” (Figure 4). Such moiré patterns are produced by the interference of crystal lattices between two twisted thin crystals, which also indicates that the powder from the activated electrodes consists

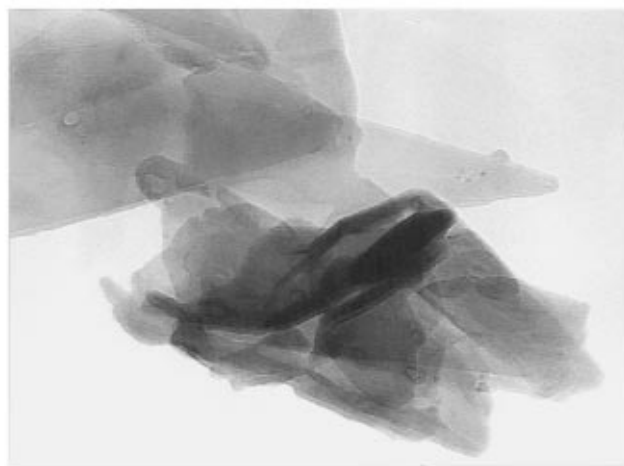


**Figure 3.** TEM image of powder scratched out of the surface of the activated *n*-TiO<sub>2</sub> electrode.

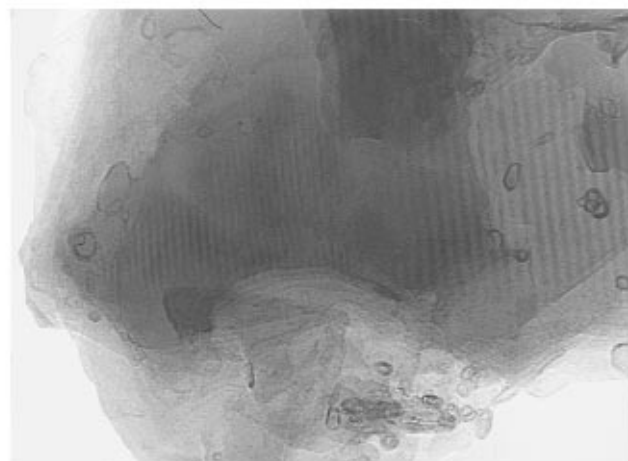


**Figure 4.** The same as Figure 3 for another part of powder.

of thin leaves of crystals. On the other hand, the scratched powder from the nonactivated electrodes consisted of fine grains having many pointed thorns (Figure 5). The thorns showed clear lattice patterns when inspected at a higher magnification ( $\times 500\,000$ ), indicating that they are in the crystalline form.

The above result can be explained if we assume that a number of atomic gaps, such as those shown schematically in Figure 6, are formed at the *n*-TiO<sub>2</sub> surface within the aforementioned micropores for the activated electrode. The atomic gaps are true “atomic-level” gaps, and they could not be detected by inspection of a cross section of the activated electrode with a Hitachi S-5000 high-resolution scanning electron microscope having a 0.6-nm resolution. Such atomic gaps will act as beginnings (or seeds) for crystal cleavage when the surface was scratched, thus resulting in thin leaves of crystals. If there are no such atomic gaps, the electrode surface is only cleaved by force upon scratching, and hence it is expected that grains with many pointed thorns are formed as really observed for the nonactivated electrode (Figure 5). The reason for the formation of the atomic gaps in the activated *n*-TiO<sub>2</sub> surface will be discussed in the discussion section.



**Figure 5.** TEM image of powder scratched out of the surface of the nonactivated *n*-TiO<sub>2</sub> electrode.

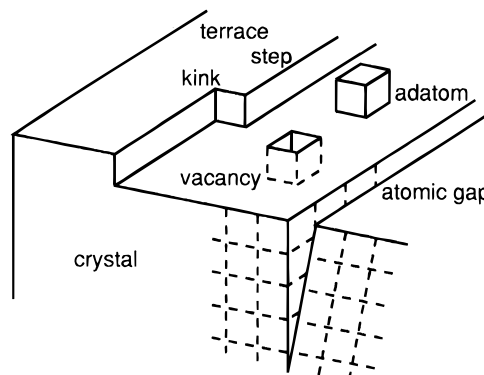
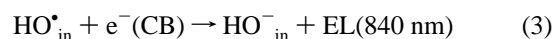
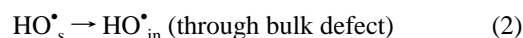
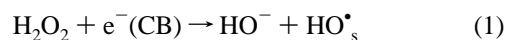


**Figure 6.** Schematic illustration of an atomic gap (a bulk defect) near the surface, together with other surface defects.

**Chemical Structure and Properties of the PL-Emitting Species.** On the basis of above result, we can expect that Ti—OH group in the atomic gaps (Figure 7) corresponds to the bulk species Ti—OH<sub>in</sub> or OH<sup>−</sup><sub>in</sub> in Figure 1. In order to get support for this model, we investigated the electroluminescence (EL) from the *n*-TiO<sub>2</sub> electrode caused by H<sub>2</sub>O<sub>2</sub>. The observed EL had the same spectrum as that of the PL band at 840 nm, showing that the EL-emitting species is the same as the PL-emitting species.

It is usually discussed in the literature<sup>22,23</sup> that the EL is emitted by a mechanism of hole injection. For example, the EL caused by H<sub>2</sub>O<sub>2</sub> is reported<sup>22,23</sup> to be emitted by hole injection by HO• radicals which were produced by reduction of H<sub>2</sub>O<sub>2</sub> by electrons in the conduction band. However, we reported in our previous papers<sup>13,15</sup> that the EL caused by H<sub>2</sub>O<sub>2</sub> is emitted by another mechanism (i.e., by the migration of the HO• radicals produced near the surface into the bulk defect (cf. Figure 7). This is because the EL intensity caused by H<sub>2</sub>O<sub>2</sub> is



much higher than that caused by S<sub>2</sub>O<sub>8</sub><sup>2−</sup>,<sup>13,15</sup> though the oxidizing power of the HO• radicals is much weaker than that

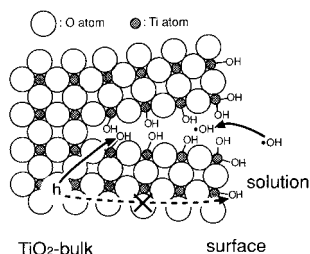


**Figure 7.** A more detailed (schematic) illustration of the atomic gap, together with some electrode processes.

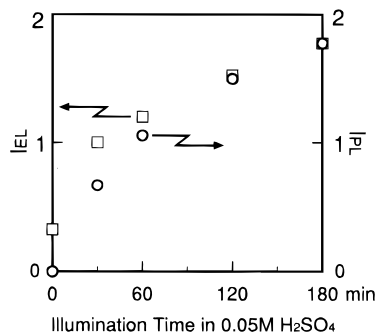


**Figure 8.** Correlation between the EL intensity ( $I_{EL}$ ) and the PL intensity ( $I_{PL}$ ).

of  $\text{SO}_4^{\bullet-}$  radicals,<sup>22,23</sup> the latter of which are produced by the reduction of  $\text{S}_2\text{O}_8^{2-}$  similar to eq 1. If both the ELs were emitted by the hole injection mechanism, the EL caused by  $\text{S}_2\text{O}_8^{2-}$  should be much stronger than that caused by  $\text{H}_2\text{O}_2$ .

In the present work, the above mechanism (eqs 1–3) was confirmed by the following experiments. We illuminated a fresh  $n\text{-TiO}_2$  electrode in 0.05 M  $\text{H}_2\text{SO}_4$  for a certain period of time for activation and then measured the EL intensity caused by  $\text{H}_2\text{O}_2$  with the electrode. Figure 2B shows the EL intensity ( $I_{EL}$ ) together with the cathodic current density ( $j_c$ ). The  $I_{EL}$  increased with the illumination time in 0.05 M  $\text{H}_2\text{SO}_4$  (i.e., the electrode activation), though the  $j_c$  was rather independent of the illumination (activation). The increase in  $I_{EL}$  can easily be explained by the increase in the number of the bulk defect (atomic gaps) on the basis of the mechanism of eqs 1–3, which in turn confirms this mechanism. Figure 8 shows the correlation between the  $I_{EL}$  and the PL intensity  $I_{PL}$ , the latter of which represents the extent of the electrode activation. The good correlation confirms the above argument (eqs 1–3). This result strongly suggests that the EL-emitting species (or the PL-emitting species) is assigned to  $\text{HO}^{\bullet}_{in}$  in the bulk defect, in harmony with our previously proposed model.

Another support to our model (Figure 1) is given by the quenching of the PL band at 840 nm by a reductant such as hydroquinone ( $\text{H}_2\text{Q}$ ) added to the solution. The quenching is explained by the reduction of  $\text{HO}^{\bullet}_{in}$  radicals (the PL-emitting species) by the reductant (cf. Figure 1). Thus, if the PL-emitting species is an intermediate of the photooxidation reaction of water, the oxygen photoevolution should also be suppressed by the reductant. Detailed experiments were made in the present work, and Figure 9 shows the correlation between the (normalized) PL intensity and the oxygen photoevolution efficiency (reported by Fujishima et al.<sup>24</sup>) as a function of the redox potential of a reductant added. The good correlation clearly shows that the PL-emitting species is an intermediate of the photooxidation reaction of water.

**PL-Emitting Species Lying in a Bulk Defect.** As reported in our previous papers,<sup>13,15</sup> the transient luminescence as well as the transient cathodic current are observed around +0.1 V

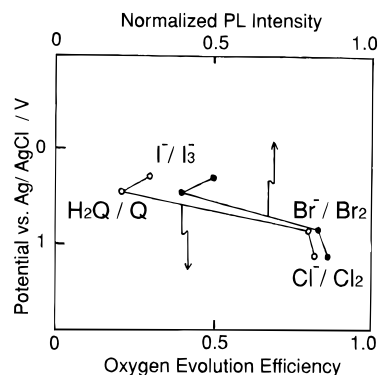


**Figure 9.** The normalized PL intensity and the oxygen photoevolution efficiency in 0.05 M  $\text{H}_2\text{SO}_4$  in the presence of a reductant, plotted as a function of the redox potential of the reductants.

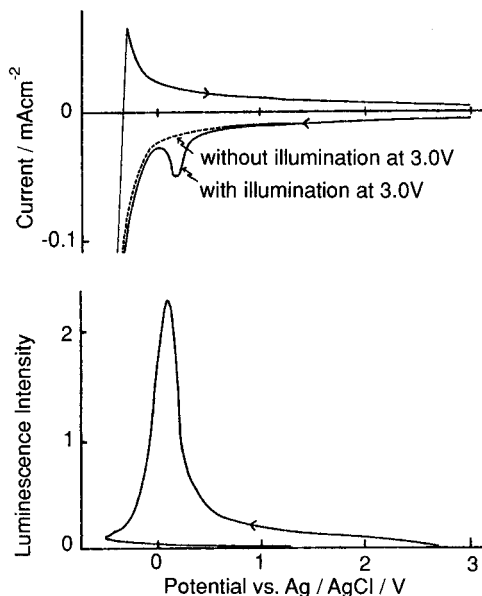


**Figure 10.** An example of the transient luminescence and the transient cathodic current observed after illumination at 3.0 V in 0.05 M  $\text{H}_2\text{SO}_4$ . See text for details.

vs  $\text{Ag}/\text{AgCl}$  (cf. Figure 10) when the  $n\text{-TiO}_2$  electrode was illuminated at a large anodic potential, say, 3.0 V, for a sufficient period of time (600 s) and then the potential was scanned in the dark toward the negative at a high rate of 0.5 V/s. The transient luminescence (TL) showed the same spectrum as the PL band at 840 nm,<sup>13</sup> showing that the TL-emitting species is the same as the PL-emitting species. The TL was explained<sup>13,15</sup> as due to a radiative recombination between a surface reaction intermediate accumulated by illumination at 3.0 V and the electrons in the conduction band.

On the basis of this result, in the present work we measured the decay rate of the reaction intermediate. The experiment was done as follows: The electrode was first illuminated at 3.0 V, and, after stopping the illumination, it was kept in the dark for a certain period of time, denoted by  $t_{\text{dark}}$ , at the same potential, and then the potential was scanned toward the negative at a rate of 0.5 V/s. Figure 11 plots the observed transient luminescence intensity ( $I_{TL}$ ) as a function of the square root of  $t_{\text{dark}}$ . The good linear  $I_{TL}$  vs  $t_{\text{dark}}^{1/2}$  relation was obtained, except for that part due to very large  $t_{\text{dark}}$ . Because the mean diffusion length of a species is in proportion to the square root of time, this result indicates that the luminescent species lying in the  $n\text{-TiO}_2$  bulk near the surface decays by diffusion to the surface.

In order to confirm the above conclusion, we examined the effect of addition of  $2.5 \times 10^{-3}$  M hydroquinone ( $\text{H}_2\text{Q}$ ) to the

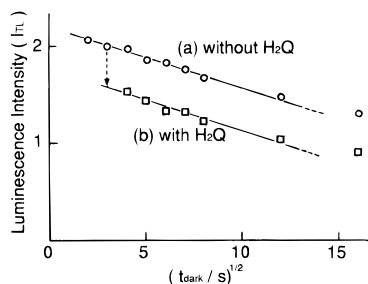


**Figure 11.** The transient luminescence intensity ( $I_{TL}$ ) vs the square root of  $t_{dark}$ : (a) is for 0.05 M  $H_2SO_4$  without hydroquinone ( $H_2Q$ ) and (b) for 0.05 M  $H_2SO_4$  with  $2.5 \times 10^{-3}$  M  $H_2Q$ . See text for details.

solution. The  $H_2Q$  in the solution can react not only with the reaction intermediate ( $HO^\bullet$  radicals) but also with the holes in the valence band of  $n$ - $TiO_2$ . Therefore, in order to see only the effect on the reaction intermediate,  $H_2Q$  was added *just after stopping the illumination at 3.0 V* in the above experiment. This was a troublesome experiment because we had to use a new electrolyte solution for each  $t_{dark}$ . The correction for a slight change in the observed  $I_{TL}$  in each experimental run, arising from a slight change in the cell and electrode positions upon renewal of the solution, was made by measuring first the  $I_{TL}$  in the absence of  $H_2Q$  for  $t_{dark} = 3$  s and then measuring the  $I_{TL}$  in the presence of  $H_2Q$  for certain  $t_{dark}$ . The latter  $I_{TL}$  values were normalized by the former  $I_{TL}$ . The introduction of  $H_2Q$  into the cell was carried out using a syringe so as not to change the cell and electrode positions.

As seen in Figure 11, the  $I_{TL}$  in the presence of  $H_2Q$  is smaller than that in the absence of  $H_2Q$  by a constant amount, but the good linear  $I_{TL}$  vs  $t_{dark}^{1/2}$  relation is still obtained with the same slope as in the case of no  $H_2Q$ . The constant decrease in  $I_{TL}$  can be explained by considering that a part of the luminescent species lying very close to the electrode surface was instantly reduced upon addition of  $H_2Q$ . The same slope as the case of no  $H_2Q$  implies that the above-mentioned diffusion of the luminescent species occurs *within* the  $n$ - $TiO_2$  crystal, not along the surface. This result also shows that the diffusion occurs along the narrow atomic gaps into which a  $H_2Q$  molecule cannot penetrate. This gives confirmative evidence to our model that the luminescent species lies in the bulk of  $n$ - $TiO_2$ .

Similar experiments were done using  $Br^-$  and  $Cl^-$  ions as a reductant instead of  $H_2Q$ , but almost no quenching of the transient luminescence was observed for such reductants. Furthermore, similar experiments were done for the decay rate of the transient cathodic current ( $j_{TC}$ ) (cf. Figure 10). The  $j_{TC}$  vs  $t_{dark}^{1/2}$  plots gave good straight lines,<sup>25</sup> but the slope was about half that for the  $I_{TL}$  vs  $t_{dark}^{1/2}$ . It is to be noted also in Figure 10 that the potential at the transient luminescence peak is about 0.06 V more negative than that at the transient cathodic current peak. These results suggest that the transient cathodic current includes contributions of the reduction of reaction intermediates (such as  $H_2O_2$ ) other than the luminescent species.

## Discussion

We have in the present work given experimental evidence to the following facts: (1) A bulk defect (atomic gaps) acting as an active reaction site is formed in the course of illumination (photoetching) of fresh  $n$ - $TiO_2$  in  $H_2SO_4$  (Figures 2A and 3–5), (2) the PL-emitting species is a bulk species (or a species in the atomic gaps) (Figure 11, especially the result in the presence of  $H_2Q$ ), (3) the PL-emitting species is an intermediate of the photooxidation reaction of water (Figure 9), and (4) the PL-emitting species is assigned to  $HO^\bullet$  radicals (Figures 2B and 8 and eqs 1–3).

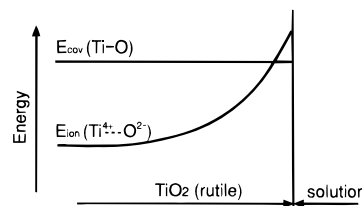


**Figure 12.** Schematic illustration for explaining a change in the ionicity of the Ti–O bond from the bulk to the surface in  $TiO_2$  (rutile) crystal.

These results give confirmative evidence to our new mechanism that the photooxidation reaction of water on  $n$ - $TiO_2$  (rutile) in acidic solutions is initiated by the oxidation of Ti–OH (or  $OH^-$ ) in a bulk defect near the surface by photogenerated holes. The assumption that surface Ti–OH species can be oxidized by holes is incompatible with the above facts 2 and 3. This assumption is also denied by the reported result that the effect of alcohols added to the solution can be explained completely by the two competitive processes by holes: the oxidation of adsorbed alcohols and the formation of the PL-emitting species,<sup>21</sup> because it has been verified in the present work that the PL- or EL-emitting species is a bulk species (Figure 11). As to the PL- or EL-emitting species, Salvador et al. suggested adsorbed  $H_2O_2$  molecules as a possible candidate,<sup>26</sup> but this possibility had no experimental support as reported previously,<sup>15</sup> because the TL such as shown in Figure 10 was not observed even in the presence of high-concentration (0.5 M)  $H_2O_2$  unless the  $n$ - $TiO_2$  electrode had beforehand been illuminated under anodic bias.

Now let us consider the reason why the atomic gaps are produced in the course of photoetching of fresh  $n$ - $TiO_2$  electrodes in 0.05 M  $H_2SO_4$ . This can be explained by taking account of the presence of a strain at (or near) the surface of the  $TiO_2$  crystal due to a large change in the ionicity of the Ti–O bond from the bulk to the surface. Figure 12 schematically explains the change in the bond ionicity. The true wave function for a Ti–O bond,  $\Psi(Ti-O)$ , can be expressed, in the first approximation, by a linear combination of the wave function of a purely ionic bond,  $\Phi_{ion}(Ti^{4+}\cdots O^{2-})$ , and that of a purely covalent bond,  $\Phi_{cov}(Ti-O)$ . The covalent bonding arises from

$$\Psi(Ti-O) = a \Phi_{ion}(Ti^{4+}\cdots O^{2-}) + b \Phi_{cov}(Ti-O) \quad (4)$$

a local interaction between atoms, and therefore, the energy for  $\Phi_{cov}(Ti-O)$ ,  $E_{cov}(Ti-O)$ , is expected to be nearly constant from the bulk to the surface. On the other hand, the energy for  $\Phi_{ion}(Ti^{4+}\cdots O^{2-})$ ,  $E_{ion}(Ti^{4+}\cdots O^{2-})$ , in the bulk is much lower than that at (or near) the surface because the effective Madelung constant at the surface is only a half of the Madelung constant for the bulk. This effect is very important for the  $TiO_2$  (rutile) crystal because it has a very large Madelung constant of 4.816.<sup>27</sup> This value can be compared with a Madelung constant for a NaCl crystal of 1.748. Thus, we can expect that the ionicity in the Ti–O bond at the surface becomes much smaller than that in the bulk.

The change in the bond ionicity will cause a change in the Ti–O distance. It is reported<sup>27</sup> that the Ti–O distance in the rutile crystal is 0.1944 and 0.1988 nm, only slightly smaller than the sum (0.206 nm) of the ionic radius of  $Ti^{4+}$  (0.060 nm) and that of  $O^{2-}$  (0.146 nm). This implies that the Ti–O bonding in the bulk is nearly ionic with a small contribution of the covalent character. On the other hand, the Ti–O distance for a molecule, for example,  $[Ti(OMe)_4]_4$  (a tetramer of  $Ti(OMe)_4$  where Me is  $CH_3$ ), is reported to be 0.177 nm for the Ti–OMe bond,<sup>28</sup> which is considerably smaller than the value of the rutile

crystal. Such a decrease in the bond distance can be attributed to an increase in the covalent bond character in the Ti—OMe bond.

From the above argument, we can expect that the Ti—O distance in the TiO<sub>2</sub> (rutile) crystal decreases from the bulk to the surface due to the decrease in the bond ionicity, and hence the crystal has a large strain at (or near) the surface. Such a strain may be released either by occurrence of crystal distortion or by formation of atomic gaps near the surface in the course of appropriate surface treatments. The formation of the atomic gaps (Figures 6 and 7) during the photoetching in 0.05 M H<sub>2</sub>SO<sub>4</sub> can be regarded as an example of such surface reconstruction.

Figure 6 shows schematically various types of surface defects. It has often been reported that surface defects such as step, kink, adatom, and vacancy act as active reaction sites. The present work has indicated that atomic gaps also act as an important active reaction site. Further detailed studies along this line may lead to finding of new active electrode materials.

## References and Notes

- (1) Trasatti, S.; O'Grady, W. E. *Adv. Electrochem. Electrochem. Eng.* **1981**, *12*, 177.
- (2) Honda, K.; Fujishima, A. *Nature (London)* **1972**, *238*, 37.
- (3) Augustynski, J. *Struct. Bonding (Berlin)* **1988**, *69*, 1 and references cited herein.
- (4) Salvador, P. *New J. Chem.* **1988**, *12*, 35.
- (5) Norton, A. P.; Bernasek, S. L.; Bocarsly, A. B. *J. Phys. Chem.* **1988**, *92*, 6009.
- (6) Kasinski, J. J.; Gomez-Jahn, L. A.; Faran, K. J.; Gracewski, S. M.; Dwayne Miller, R. J. *J. Chem. Phys.* **1989**, *90*, 1253.
- (7) Kiwiet, N. J.; Fox, M. A. *J. Electrochem. Soc.* **1990**, *137*, 561.
- (8) Nogami, G.; Sei, H.; Aoki, A.; Ohkubo, S. *J. Electrochem. Soc.* **1994**, *141*, 3410.
- (9) Salama, S. B.; Natarajan, C.; Nogami, G.; Kennedy, J. H. *J. Electrochem. Soc.* **1995**, *142*, 806.
- (10) Kratochvilova, K.; Hoskocova, I.; Jirkovsky, J.; Klima, J.; Ludvik, J. *Electrochim. Acta* **1995**, *40*, 2603.
- (11) Shaw, K.; Christensen, P.; Hamnett, A. *Electrochim. Acta* **1996**, *41*, 719.
- (12) Nosaka, Y.; Koenuma, K.; Ushida, K.; Kira, A. *Langmuir* **1996**, *12*, 736.
- (13) Nakato, Y.; Tsumura, A.; Tsubomura, H. *J. Phys. Chem.* **1983**, *87*, 2402.
- (14) Nakato, Y.; Tsumura, A.; Tsubomura, H. *Chem. Phys. Lett.* **1982**, *85*, 387.
- (15) Nakato, Y.; Ogawa, H.; Morita, K.; Tsubomura, H. *J. Phys. Chem.* **1986**, *90*, 6210.
- (16) Nakato, Y.; Tsubomura, H. *Denki Kagaku oyobi Kogyo Butsuri Kagaku* **1989**, *57*, 1108.
- (17) The (medium) reorganization energy ( $\lambda$ ) can be calculated approximately by an equation  $\lambda = (e^2/8\pi a\epsilon_0)(1/\epsilon_{op} - 1/\epsilon_s)$  where  $e$  is the elementary charge,  $a$  is the effective radius (or van der Waals radius) of the species (OH<sup>-</sup> ion),  $\epsilon_0$  is the permittivity of vacuum, and  $\epsilon_{op}$  and  $\epsilon_s$  are the optical and static dielectric constants respectively, according to Marcus theory (Marcus, R. A. *Ann. Rev. Phys. Chem.* **1964**, *15*, 155). Thus, the  $\lambda$  value for the oxidation of bulk Ti—OH or OH<sup>-</sup> species is calculated to be only 0.7 eV, whereas that for aqueous OH<sup>-</sup> ions is calculated to be 2.44 eV by taking  $a = 0.16$  nm,<sup>16</sup>  $\epsilon_{op}$  (water) = 1.8,  $\epsilon_s$  (water) = 78,  $\epsilon_{op}$  (TiO<sub>2</sub>) = 6.4, and  $\epsilon_s$  (TiO<sub>2</sub>) = 117.<sup>27</sup> The  $\lambda$  value for the oxidation of surface Ti—OH or OH<sup>-</sup> species is estimated to be about 1.6 eV as an average of the values for the solid bulk and aqueous species, which is much larger than the value (0.7 eV) for the solid bulk species.
- (18) Grabner, L.; Stokowski, S. E.; Brower, W. S., Jr. *Phys. Rev. B* **1970**, *2*, 590.
- (19) Smandek, B.; Gerischer, H. *Electrochim. Acta* **1989**, *34*, 1411.
- (20) Nakato, Y.; Akanuma, H.; Shimizu, J. -I.; Magari, Y. *J. Electroanal. Chem.* **1995**, *396*, 35.
- (21) Magari, Y.; Ochi, H.; Yae, S.; Nakato, Y. Solid/Liquid Electrochemical Interfaces; ACS Symposium Series 656; American Chemical Society, Washington, DC, 1996; Chapter 21.
- (22) Beckmann, K. H.; Memming, R. *J. Electrochem. Soc.* **1969**, *116*, 368.
- (23) Pettinger, B.; Schoeppel, H. -R.; Gerischer, H. *Ber. Bunsen-Ges. Phys. Chem.* **1976**, *80*, 849.
- (24) Fujishima, A.; Inoue, T.; Honda, K. *J. Am. Chem. Soc.* **1979**, *101*, 5582.
- (25) A similar square-root-of-time dependence of the transient cathodic current is reported for sintered *n*-SrTiO<sub>3</sub>, for example, see: Salvador, P.; Gutierrez, C. *J. Electroanal. Chem.* **1984**, *160*, 117.
- (26) Salvador, P.; Gutierrez, C. *J. Phys. Chem.* **1984**, *88*, 3696.
- (27) Grant, F. A. *Rev. Mod. Phys.* **1959**, *31*, 646.
- (28) McAuliffe, C. A.; Barratt, D. S. *Comprehensive Coordination Chemistry, The Synthesis, Reactions, Properties & Applications of Coordination Compounds*, 1st ed.; Sir Wilkinson, G., Ed.; Pergamon Press: New York, **1987**; Vol. 3, p 333.